Numerical Investigations on the Whistling Ability of a Single Hole Orifice in a Flow Duct

Romain Lacombe, Stephan Föller, Gary Jasor, Wolfgang Polifke, Yves Aurégan, Pierre Moussou

10ème **C**ongrès **F**rançais d'**A**coustique

Lyon, 12-16 Avril 2010

Numerical Investigations on the Whistling Ability of a Single Hole Orifice in a Flow Duct

R. Lacombe[1], S. Föller[2], G. Jasor[2], W. Polifke[2], Y. Aurégan[3], P. Moussou[1]

[1] LaMSID, UMR EDF-CNRS 2832, 1, Av. du Général de Gaulle, 92141 Clamart Cedex, France, romain.lacombe@edf.fr

[2] Lehrstuhl für Thermodynamik, Technische Universität München, Garching, D-85747, Germany

[3] Laboratoire d'Acoustique de l'Université du Maine, UMR CNRS 6613, Avenue Olivier Messiaen, 72085 Le Mans Cedex 9, France

The study focuses on characterizing the whistling ability of an axisymmetric orifice in confined flow, using numerical simulation and system identification method.
A single hole orifice in a duct can generate a whistling when it is submitted to a low Mach number flow. This whistling is a consequence of acoustic amplification downstream of the orifice. This amplification is a necessary, but not sufficient condition to generate whistling, a feedback loop is also needed. The present study deals with characterizing the acoustic amplification of such a device. A Large Eddy Simulation (LES) is performed for an orifice submitted to a low Mach number turbulent flow. Broadband acoustic signals are applied to the inlet and to the outlet of the computational domain. The extracted acoustic time series of the LES are post-processed with the Wiener-Hopf Inversion technique to obtain the coefficients of the scattering matrix in the linear regime. The resulting scattering matrix is used to compute a whistling criterion. This energy criterion defines the frequencies, at which an acoustic amplification may occur and so characterizes the whistling ability of the orifice. This criterion has previously been successfully applied to single hole orifices in a test rig.
Comparisons between experimental and numerical results, at two different Mach numbers, show a good agreement up to a limit frequency. By applying the whistling criterion, the potential whistling frequency range is well predicted in terms of frequency and amplitude. A second potential whistling frequency range is predicted, for one flow configuration, whereas it is observed in the experiments at higher frequencies.

1 Introduction

A sharp edge orifice in a flow duct, with acoustic reflections on both sides, is known to whistle under certain flow regimes. For example in pipe systems of power plant, where orifices are used as measurement devices or pressure drop devices, whistling phenomena have been observed. In addition to a high noise level, the whistling can lead to a risk of fatigue failure of the pipe due to strong vibration levels.

The whistling is known to be a consequence of self-sustained oscillations in pipe systems [1, 2]. Shear flow instability, downstream of the orifice, plays the role of an amplifier for incident acoustic perturbations. The presence of acoustic reflections upstream and downstream of this area offers a feedback, so that the perturbations are reflected back to the amplification area. Thus, self-sustained acoustic oscillations are created. When the limit cycle is reached, non-linear effects set the amplitude and the frequency of the whistling.

In a previous work [3], an experimental characterization of the whistling ability of a large number of orifices has been done. One of the results of this work was the definition of an acoustic power criterion used to define the potential whistling frequencies.

The goal of the present paper is to characterize the whistling ability of an orifice from a compressible flow simulation. The idea is to extract the scattering matrix of the singularity from a simulation and then to utilize the acoustic power criterion. This procedure is applied for two flow conditions.

To compute the scattering matrix, a two step process is used [4, 5]. First, a compressible flow simulation is done with superimposed broadband acoustic excitations. Then, a system identification method allows to extract the scattering matrix of the orifice.

In a first section, a brief review of the whistling criterion is presented. Then, the method, which is used to extract the scattering matrix of the orifice from a LES, is introduced. In a third section, the two studied cases are defined, followed by a short presentation of the numerical tool. Finally, the results are shown and compared with experimental data. The comparisons are made in terms of the scattering matrix and the whistling ability.

2 The whistling criterion

First, a brief review of a whistling criterion, which is used to characterize the whistling ability of an orifice, is presented.

As mentioned in the introduction, the shear flow instability downstream of the orifice can amplify an incident acoustic perturbation. Thus, due to a modulation of the vorticity in the shear layer, a part of the energy of the mean flow can be transferred into acoustic

waves. The potential whistling frequencies of the orifice can be identified, by characterizing the frequencies where acoustic amplification occurs.

As Aurégan and Starobinsky introduced in a case of an acoustic multiport [6], this idea has been used by Testud *et al.* [3]. In their work, they defined the minimum and maximum dissipated acoustic power at the orifice from the coefficients of the scattering matrix. At frequencies with a negative minimum of the dissipated acoustic power, acoustic amplification can occur. The frequencies are then defined as potential whistling frequencies.

The application of the criterion needs the knowledge of the scattering matrix of the orifice, which was previously determined experimentally. In this paper, the determination of this matrix is performed from a turbulent flow simulation. The next section presents the method used to determine the scattering coefficients.

3 The LES/SI Method

In this section, the numerical procedure is introduced. It is based on a single compressible flow simulation and an adjacent acoustic signal analysis. Then, from acoustic pressure and velocity times series, the acoustic scattering matrix is determined using a system identification method, so-called Wiener-Hopf Inversion. This overall procedure is called LES/SI [4, 5]. A scheme of the method is depicted in figure 1.

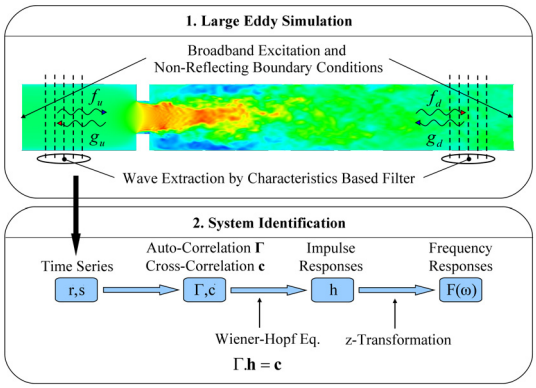

Figure 1: LES/SI Method.

First, a three-dimensional compressible LES of the studied case is performed. Broadband acoustic excitations are simultaneously applied upstream and downstream of the orifice. The excitation signals are two statistically independent Pseudo Random Binary Signals (PRBS), which randomly switch between two discrete values. This signal is chosen for its property of good decorrelation with itself, which is known to be helpful for the application of the Wiener-Hopf Inversion. In addition, non-reflecting boundary conditions need to be enforced at the inlet and at the outlet [7, 8].

At different planes upstream and downstream of the orifice, space averaged pressure and velocity are recorded with a fixed time step. The acoustic variables p' and u' are extracted from this instantaneous values, by subtracting the long time average and by applying a characteristic based filter [9]. This filter uses the property that acoustic plane waves propagate with the speed of sound corrected by the mean flow velocity, whereas turbulent fluctuations have a convection velocity close to the background flow velocity. The characteristic wave amplitudes f and g are then computed as

$$f = \frac{1}{2}\left(\frac{p'}{\rho c} + u'\right) \text{ and } g = \frac{1}{2}\left(\frac{p'}{\rho c} - u'\right), \qquad (1)$$

with ρ the density of the fluid at rest and c the speed of sound. Under this form, the signals and the responses of the acoustic biport are respectively f_u, g_d and g_u, f_d, where subscripts u and d denote upstream and downstream.

Under the assumption of a linear problem, *i.e.*, the system can be seen as a Linear and Time-Invariant (LTI) system, the unit-impulse response $\mathbf{h}$ characterizes the system behavior completely. Here the Wiener-Hopf is utilized to determine the unit-impulse response,

$$\mathbf{\Gamma}.\mathbf{h} = \mathbf{c}, \qquad (2)$$

with $\mathbf{\Gamma}$ the autocorrelation matrix of the signals and $\mathbf{c}$ the crosscorrelation vector between the responses and the signals. The unit-impulse response is obtained by inverting the autocorrelation matrix,

$$\mathbf{h} = \mathbf{\Gamma}^{-1}.\mathbf{c}. \qquad (3)$$

More details on the Wiener-Hopf Inversion can be found in [4, 10].

Finally, the z-transform of the unit-impulse responses gives the coefficients of the scattering matrix of the system in the frequency domain.

4 Studied configuration and flow simulation

4.1 Definition of the geometry and flow conditions

The main pipe diameter is $D = 3 \times 10^{-2}$ m. The orifice diameter is $d = 1.5 \times 10^{-2}$ m, whereas its thickness is $t = 5 \times 10^{-3}$ m. The edges of the orifice are all sharp.

Two operating flow conditions are studied. The flow parameters in the main pipe are presented in table 1.

Operating condition number	1	2
U (mean flow velocity)	9 m.s^{-1}	12 m.s^{-1}
M (Mach number)	2.6×10^{-2}	3.5×10^{-2}
Re (Reynolds number)	≈ 18000	≈ 24000

Table 1: Flow parameters of the studied operating conditions.

These configurations have been experimentally studied on the test rig at the LAUM (Laboratoire d'Acoustique de l'Université du Maine), [3, 11]. Here, the goal is to predict the whistling behavior of the orifice with the LES/SI method.

4.2 Flow simulation

The solver used in this study is AVBP, developed by CERFACS[1]. It solves the three-dimensional compressible Navier-Stokes equations on unstructured meshes, with a LES approach for the turbulence modeling. Large vortical structures of the flow field are fully resolved, whereas the small scales are modeled with the standard WALE subgrid-scale model [12]. The second order Lax-Wendroff discretization scheme is applied.

In the axial direction, the computational domain is extended over five times the main pipe diameter upstream of the orifice, for the two flow conditions, and twelve times the main pipe diameter downstream, for the flow condition 1 and eight times in the case of flow condition 2. The structured grid is made of 5.3 million cells for the configuration 1, 5.5 million cells for the configuration 2. The smallest cells have a size of 4.2×10^{-5} m for the flow condition 1, 4.3×10^{-5} m for the flow condition 2, the largest size is 9.1×10^{-4} m for the flow condition 1, 2.7×10^{-4} m for the flow condition 2. Here, frequencies up to 5000 Hz are studied. At this frequency the resolution is around 80 grid points per wavelength for the largest cells, which is sufficient. In the axial direction, the mesh is refined around the orifice, because the resolution close to the edge of the orifice appeared to be a crucial parameter, since the initial instability of the shear layer controls the aeroacoustic interaction. The contraction of the flow upstream to the orifice must be well resolved to capture the correct flow angle around the upstream edge and the strong velocity gradient at this point. In the radial direction, the grid size is refined at the orifice wall and in the area of the jet downstream of the orifice. Fine grid resolution is also required close to the walls of the main pipe, in order to capture the upstream separation point accurately.

As specified in section 3, two statistically independent acoustic excitations are applied to the inlet and to the outlet of the computational domain.

The excitations are imposed as the time derivative of the ingoing characteristic waves amplitude f_u and g_d, respectively at the inlet and at the outlet. The amplitude of these excitations is scaled to 1.7 % of the mean flow inlet velocity, which corresponds to the amplitude used in the experiments. This level ensures a linear response of the shear layer at the orifice, *i.e.*, a response independent of the excitation level.

The total simulation time is 0.2 s, with a time step of 8×10^{-8} s. The time series used for the system identification are stored every tenth time step, *i.e.*, every 8×10^{-7} s. In order to capture all relevant time lags of the system, the length of the unit impulse responses $\mathbf{h}$, in the equation (2), has been set to 3.10^{-3} s. This time interval covers the time for the waves propagation and the interaction of the sound waves with the coherent vortex structure.

5 Results

The results of the LES/SI method are now presented and compared to experiments. First, the coefficients of the scattering matrix for the flow condition 1 are presented, then the whistling ability of the orifice, for the two operating conditions, is studied using the whistling criterion.

[1] http://www.cerfacs.fr/4-26334-The-AVBP-code.php

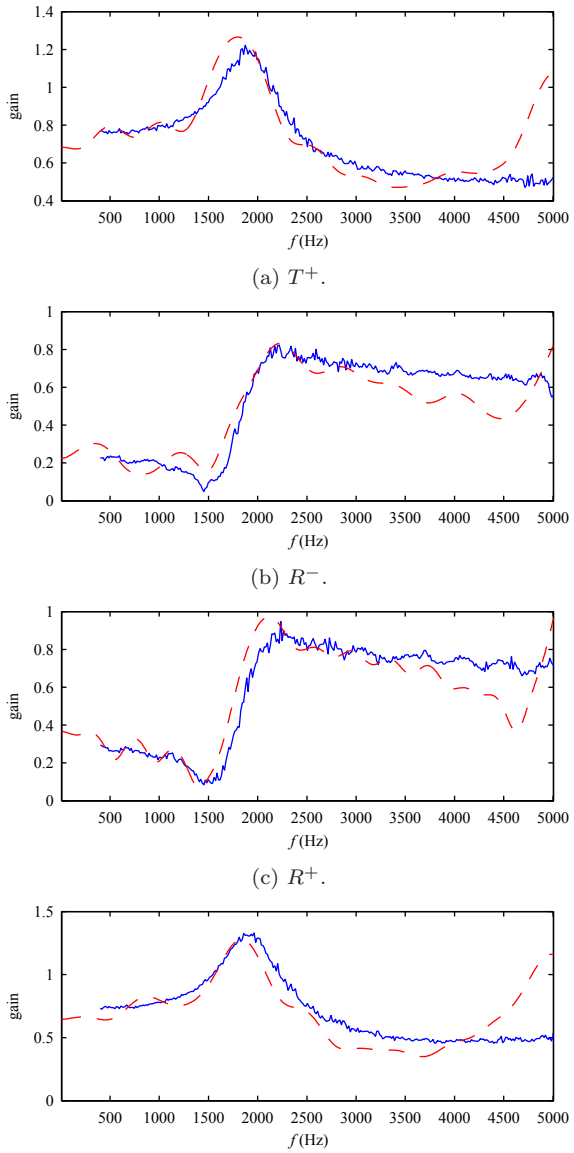

(a) T^+.

(b) R^-.

(c) R^+.

(d) T^-.

Figure 2: Absolute value of the scattering coefficients. Solid blue line: experimental results, dashed red line: numerical results.

5.1 Scattering matrix

Figures 2 and 3 respectively present the absolute value and the phase of the coefficients of the scattering matrix. Only the results for the operating condition 1 are shown.

Numerical and experimental results agree well up to 4000 Hz.

The behavior of the coefficients around 2000 Hz, *i.e.*, peaks and sharp slopes for the coefficients, are well predicted in terms of frequency and amplitude. As it will be shown in the next paragraph, this frequency range corresponds to the potential whistling frequency range.

For higher frequencies, there is a deviation between experimental data and numerical results. As it will be mentioned in the section 5.2, the behavior observed

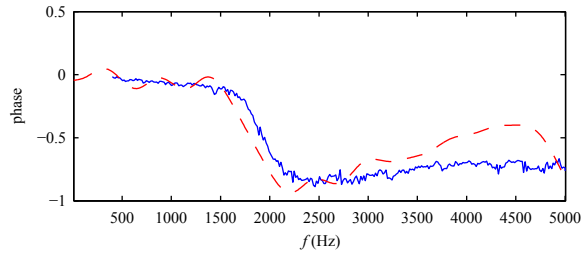

(a) T^+.

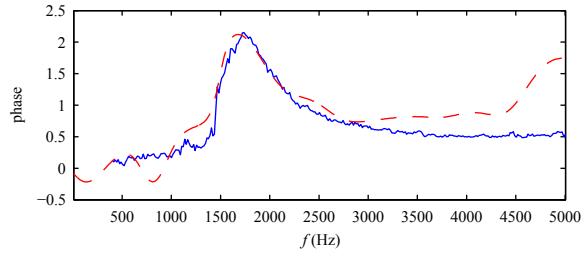

(b) R^-.

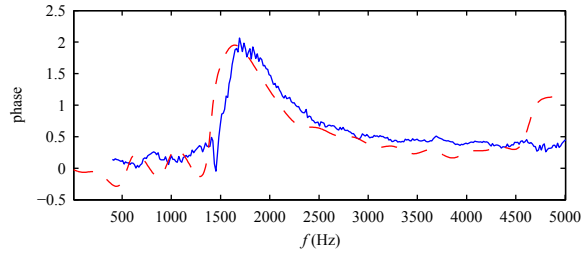

(c) R^+.

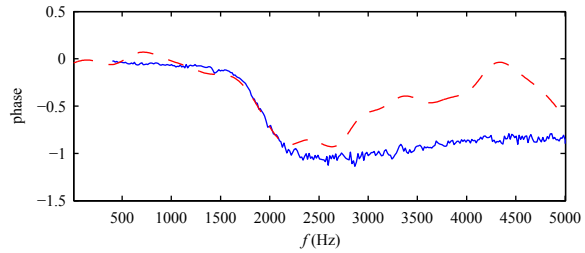

(d) T^-.

Figure 3: Phase of the scattering coefficients. Solid blue line: experimental results, dashed red line: numerical results.

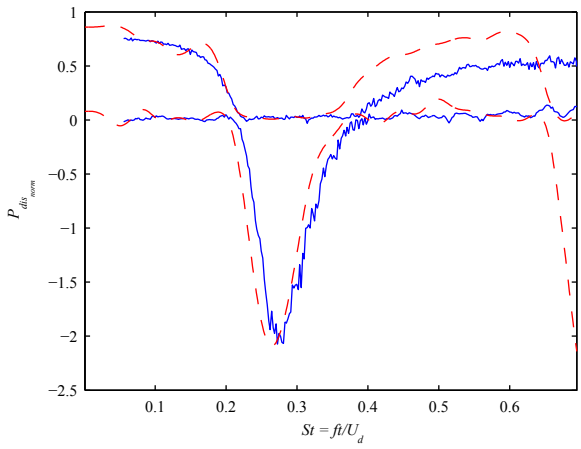

Figure 4: Maximum and minimum of the normalized dissipated acoustic power in the orifice, for an inlet velocity of 9 m.s^{-1}. Solid blue lines: experimental results, dashed red lines: numerical results.

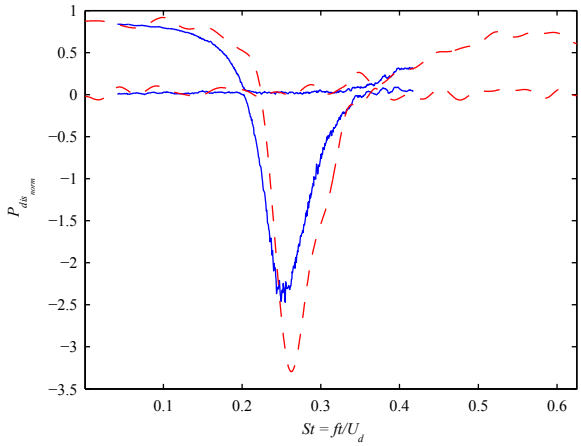

Figure 5: Maximum and minimum of the normalized dissipated acoustic power in the orifice, for an inlet velocity of 12 m.s^{-1}. Solid blue lines: experimental results, dashed red lines: numerical results.

around 5000 Hz for the numerical results corresponds to a second mode of whistling, which is also observed in the experiments, but for higher frequencies.

5.2 Study of the whistling ability

Based on the scattering matrix, the whistling criterion is derived, as introduced in section 2. The potential whistling frequencies are determined from the minimal and maximal normalized dissipated acoustic power, $P_{dis_{min}}$ and $P_{dis_{max}}$. Both of them are plotted versus a Strouhal number in figures 4 and 5, for the two operating flow conditions. This Strouhal number is based on the thickness t of the orifice and on the orifice flow velocity $U_d = U\ (D/d)^2$ [3].

At low frequency, before $St = 0.2$, the incident acoustic energy can only be dissipated: all the terms $P_{dis_{min}}$ and $P_{dis_{max}}$ are positive. For this frequency range, the agreement between the experiments and the simulation is good.

The first whistling mode is observed between $St = 0.2$ and $St = 0.35$, for the two inlet velocities. The minimum of the acoustic dissipated power is negative, which means that an incident acoustic wave can be amplified. Thus, the frequency range $0.2 < St < 0.35$ is defined as a potential whistling frequency range, following the whistling criterion. This first mode of whistling is well predicted by the simulation. A slight shift towards lower frequencies is observed for the operating condition 1, whereas a shift towards higher frequencies is noticed for the operating condition 2.

At higher frequencies, dissipation only is observed. Again, the terms $P_{dis_{min}}$ and $P_{dis_{max}}$ are positive. For this frequency range, simulation results agree with experiments up to $St = 0.6$, then the numerical results, for the flow condition 1, predict the presence of a second whistling mode. In fact, this second mode has been observed experimentally for other geometries and/or operating flow conditions, but for the present condition it appeared at higher frequencies. These observed discrep-

ancies in frequency are under investigations. Since the aeroacoustic interaction is affected by the flow field at the upstream edge, this shift might be a consequence of a too coarse mesh resolution in this area. In the present study, the wall nearest node is located at $y^+ = 4$ for the operating condition 1 and at $y^+ = 6$ for the second flow condition. Due to a large increase of the computational time for a finer resolution, the influence of a grid refinement on this shift has not been carried out.

6 Conclusion

In this work, the whistling ability of an orifice has been characterized using a numerical approach. It consists of an acoustically excited LES and an acoustic signal analysis. Here we applied the Wiener-Hopf Inversion to extract the scattering matrix of the orifice. From this matrix, the whistling ability has been studied with an acoustic power criterion. All results have been compared with previous experiments.

This method is able to characterize the whistling ability of an orifice up to a certain frequency limit. Therefore, the acoustic amplification or dissipation in the shear layer were well predicted.

The determination of the scattering matrix of the orifice could then be used in a network model, composed of reflection elements and ducts. Later configuration can be found in industrial applications. The instability frequency of this system could be investigated to predict the whistling.

Moreover, the use of a compressible flow simulation offers many possibilities. The non-linear behavior of the amplification could be investigated, *i.e.*, how non linear effects influence harmonic incident perturbations at high amplitude. Furthermore, the case of an orifice with reflecting boundary conditions can be fully studied numerically. In that case, no external excitation should be added and the system should whistle by itself. The resulting whistling could finally be studied in terms of frequency and amplitude.

References

[1] S. W. Rienstra and A. Hirschberg. *An Introduction to Acoustics*. Eindhoven University of Technology, Eindhoven, The Netherlands, 2006.

[2] D. Rockwell and E. Naudascher. Self-sustained oscillations of impinging free shear layers. *Annual Review of Fluid Mechanics*, 11:67–94, 1979.

[3] P. Testud, Y. Aurégan, P. Moussou, and A. Hirschberg. The whistling potentiality of an orifice in a confined flow using an energetic criterion. *Journal of Sound and Vibration*, 325(4):769–780, 2009.

[4] W. Polifke, A. Poncet, C. O. Paschereit, and K. Döbbeling. Reconstruction of acoustic transfer matrices by instationary computational fluid dynamics. *Journal of Sound and Vibration*, 245:483–510, 2001.

[5] S. Föller, R. Kaess, and W. Polifke. Reconstruction of the acoustic transfer matrices from large-eddy-simulations of compressible turbulent flows. In *14th AIAA/CEAS Aeroacoustics Conference*, number AIAA 2008-3046, 2008.

[6] Y. Aurégan and R. Starobinsky. Determination of acoustic energy dissipation/production potentiality from the acoustic transfer functions of a multiport. *Acustica*, 85:788–792, 1999.

[7] W. Polifke, C. Wall, and Moin P. Partially reflecting and non-reflecting boundary conditions for simulation of compressible viscous flow. *Journal of Computational Physics*, 213:437–449, 2006.

[8] R. Kaess, A. Huber, and W. Polifke. Time-domain impedance boundary condition for compressible turbulent flow. In *14th AIAA/CEAS Aeroacoustics Conference*, number AIAA 2008-2921, 2008.

[9] J. Kopitz, E. Bröcker, and W. Polifke. Characteristic-based filter for identification of planar acoustic waves in numerical simulation of turbulent compressible flow. In *12th International Congress of Sound and Vibration*, July 2005.

[10] L. Ljung. *System identification - Theory for the User*. 2nd edition, PTR Prentice Hall, Upper Saddle River, N.J., 1999.

[11] G. Ajello. *Mesures acoustiques dans les guides d'ondes en présence d'écoulement - Mise au point d'un banc de mesure - Application à des discontinuités*. PhD thesis, Laboratoire d'Acoustique de l'Université du Maine, Académie de Nantes, 1997.

[12] F. Nicoud and F. Ducros. Subgrid-scale stress modelling based on the square of the velocity gradient tensor. *Journal of Flow, Turbulence and Combustion*, 62:183–200, 1999.